Franz et al., http://www.jcb.org/cgi/content/full/jcb.201305109/DC1

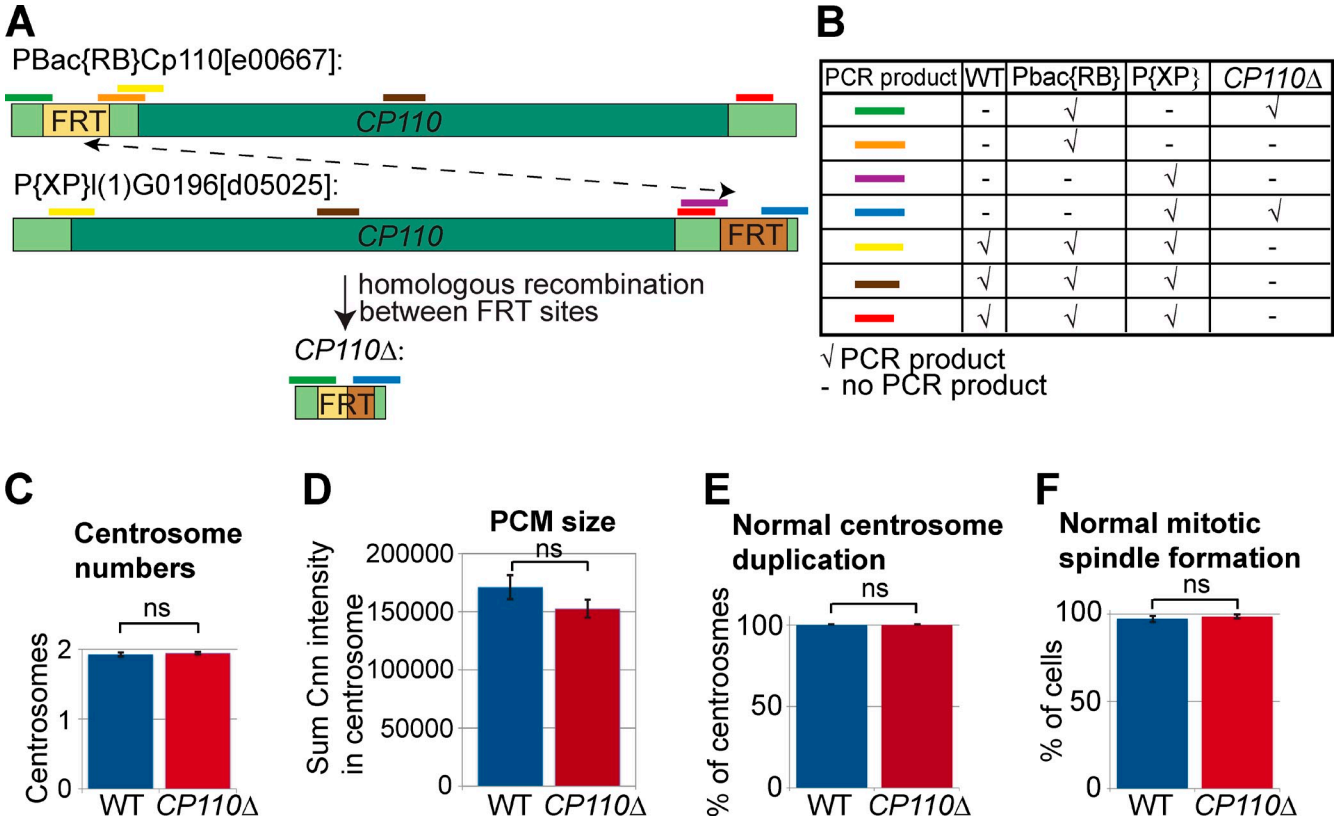

Figure S1. ***CP110Δ* mutants have no obvious defects in centriole duplication, PCM recruitment, or mitotic spindle formation.** (A) Schematic showing the scheme used to generate the *CP110Δ* mutant. Recombination between the FRT sites in PBac{RB}Cp110[e00667] and P{XP}l(1)G0196[d05025] (located in the 5′UTR and 3′UTR of *CP110*, respectively) was induced by FLP recombinase, resulting in the deletion of the entire coding region of *CP110*. Colored lines indicate the regions of the gene analyzed by PCR. (B) A summary of the PCR analyses used to confirm the deletion. DNA isolated from WT, the two original P-elements, and the putative deletion stock was tested; regions analyzed are indicated by colored bars that match those in A. (C and D) Quantification of centrosome number (C, judged by the number of Asl- and Cnn-positive dots) and PCM size (D, judged by Cnn staining) in mitotic cells from WT and *CP110Δ* third instar larval brains; *n* (total cells; total brains) = 640;15 and 742;14, respectively (C) and 140;4 and 196;5, respectively (D). (E) Quantification of the percentage of centrosomes that duplicate normally in WT and *CP110Δ* syncytial embryos expressing GFP-PACT and RFP-Cnn; *n* (total centrosomes; total embryos) = 277;4 and 413;9, respectively. (F) Quantification of the percentage of mitotic spindles that form normally in WT and *CP110Δ* syncytial embryos expressing GFP-PACT and RFP-tubulin; *n* (total cells; total embryos) = 195;6 and 228;7, respectively.

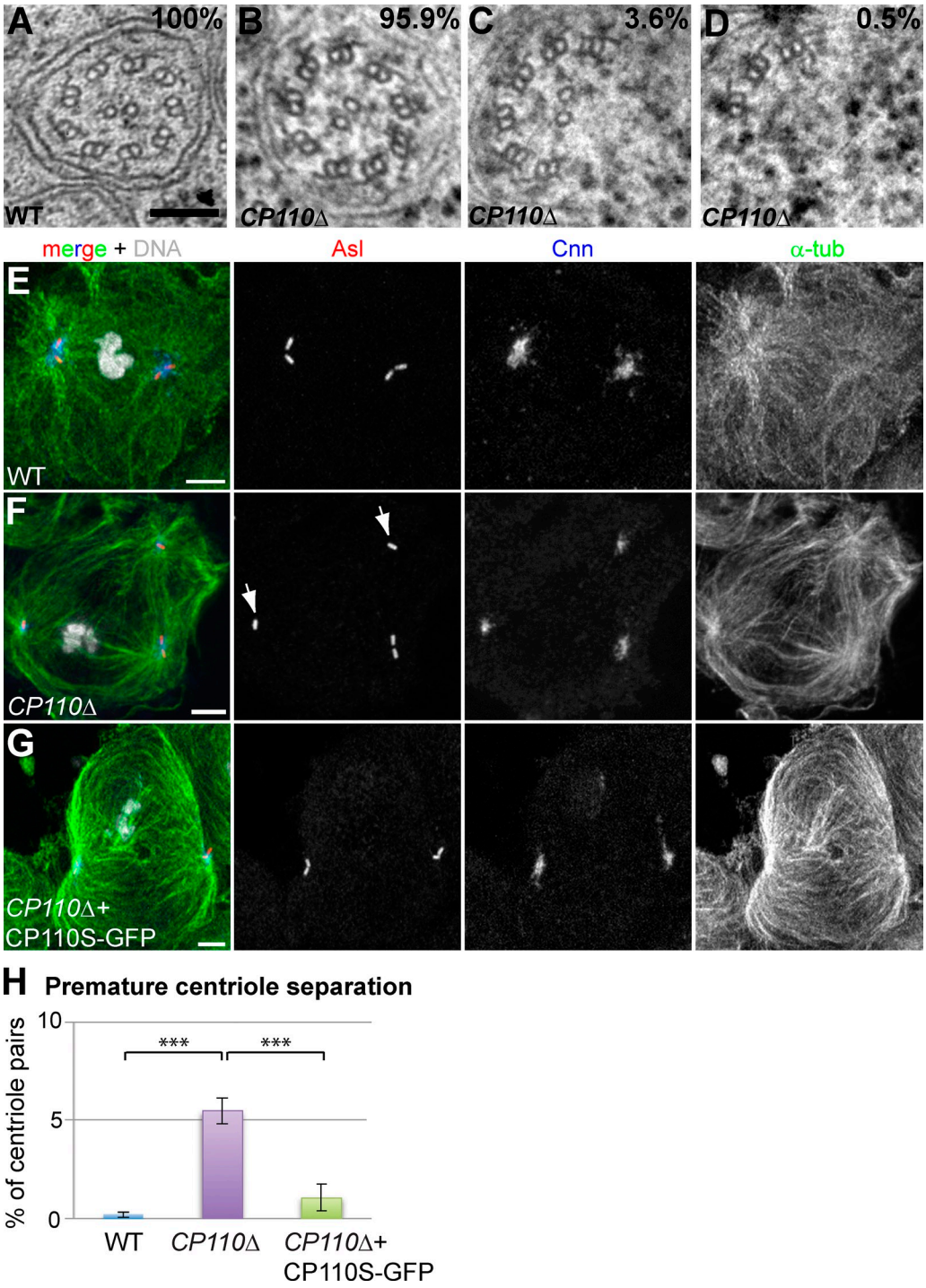

Figure S2. **Defects in axoneme ultrastructure and centriole cohesion in *CP110Δ* testes.** (A–D) Panels show EM micrographs of axonemes in WT and *CP110Δ* spermatids in cross section (n = 1,172 and 441, respectively); the percentage of axonemes missing at least one outer MT doublet (C) or the inner MT pair (D) is indicated in top right corners. (E–G) Panels show WT (E), *CP110Δ* (F), and *CP110Δ* CP110S-GFP–overexpressing (G) primary spermatocytes in meiosis I stained for Asl (red), Cnn (blue), α-tubulin (green), and DNA (white in merged image). Arrows highlight a centriole pair that has separated prematurely in the *CP110Δ* cell. (H) Quantification of premature centriole separation in WT, *CP110Δ*, and *CP110Δ* CP110S-GFP–overexpressing primary spermatocytes in late G2 phase (stained for Asl); n (total cells; total testes) = 3678;23, 6816;33, and 3486;13, respectively. Bars: (A–D) 100 nm; (E–G) 5 µm.

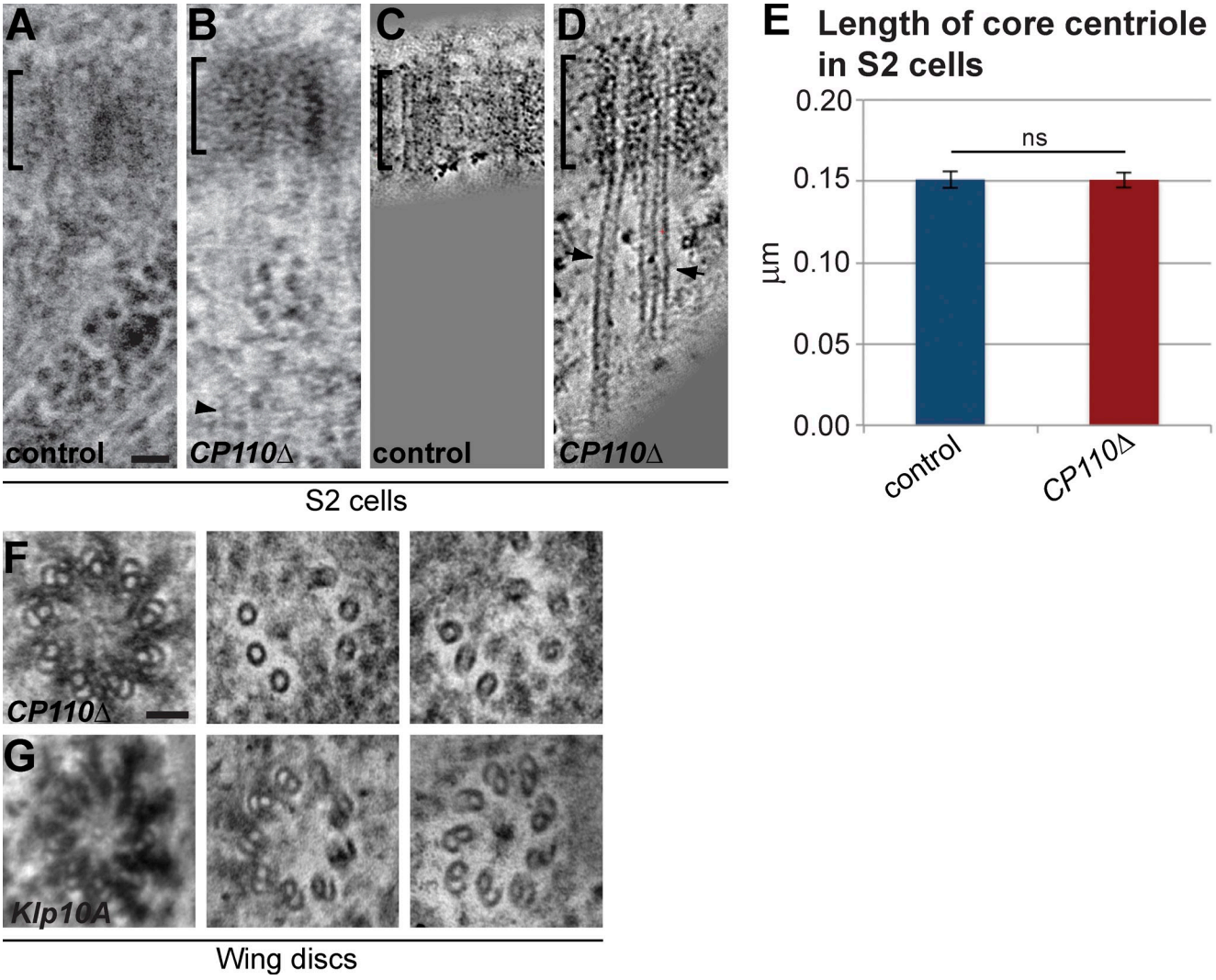

Figure S3. **An analysis of centriole microtubules in S2 cells depleted of CP110 and in wing disc cells lacking CP110 or mutant for *Klp10A*.** (A–D) Panels show representative EM images (A and B) or projections of an EM tomogram (C and D) of a centriole in S2 cells treated with RNAi against GFP (control, A and C) or CP110 (B and D). In the CP110 knockdown (confirmed by immunofluorescence and Western blotting; not depicted) centriolar MTs extend dramatically (arrows) beyond the centriole (brackets). This is much easier to see in the tomogram than in the EM section (see Video 2 for representative tomograms). *n* (total centrioles; total EM block): 24;2 (C), 26;2 (D). Interestingly, although our numbers are small ($n = 8$), roughly half of the MT extensions were singlets and half doublets. (E) Bar charts show the quantification of centriole length in S2 cells treated with RNAi against GFP (control, blue bar) or CP110 (red bar). Note that an average centriole length for 10 centrioles in each of two EM blocks (20 centrioles in total) was calculated for each treatment, and 20 was then used as the sample number for statistical analysis. We remain cautious in concluding anything about centriole length in these S2 cells, as the number of experimental replicates was too small to reliably test significance. (F and G) Panels show EM images from successive serial sections of 150-nm thickness through the centrioles and MT extensions in *CP110Δ* (F) and *Klp10A* mutant (G) third instar larval wing discs. The first sections (left panels) contain the centriole: the cartwheel and electron-dense outer appendages are visible. The second and third sections (middle and right panels) extend into the MT extensions that are mostly singlets in the case of *CP110Δ* (F) but are mostly doublets in the case of the *Klp10A* mutant (G). Bar, 50 nm.

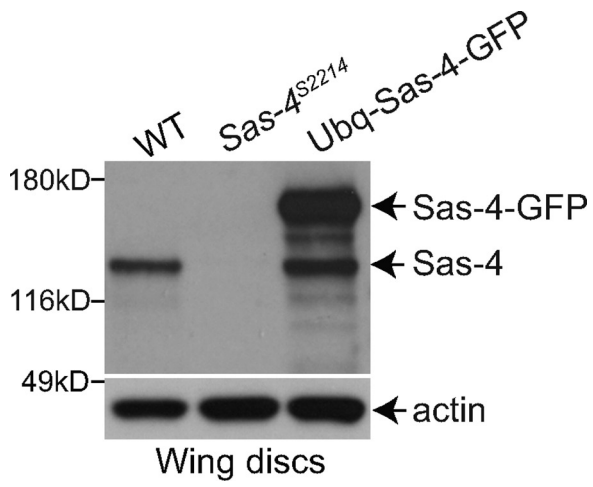

Figure S4. **Analysis of DSas-4-GFP overexpression in wing discs.** Western blots of third instar larval wing discs from WT, *DSas4*^{S2214}, or Ubq-DSas4-GFP–expressing lines were probed with anti–DSas-4 or anti-actin antibodies. Endogenous DSas-4 is expressed in WT cells and is missing in *DSas-4*^{S2214} cells. In the Ubq-DSas-4-GFP–expressing line both the endogenous DSas-4 and the overexpressed DSas-4-GFP are detected.

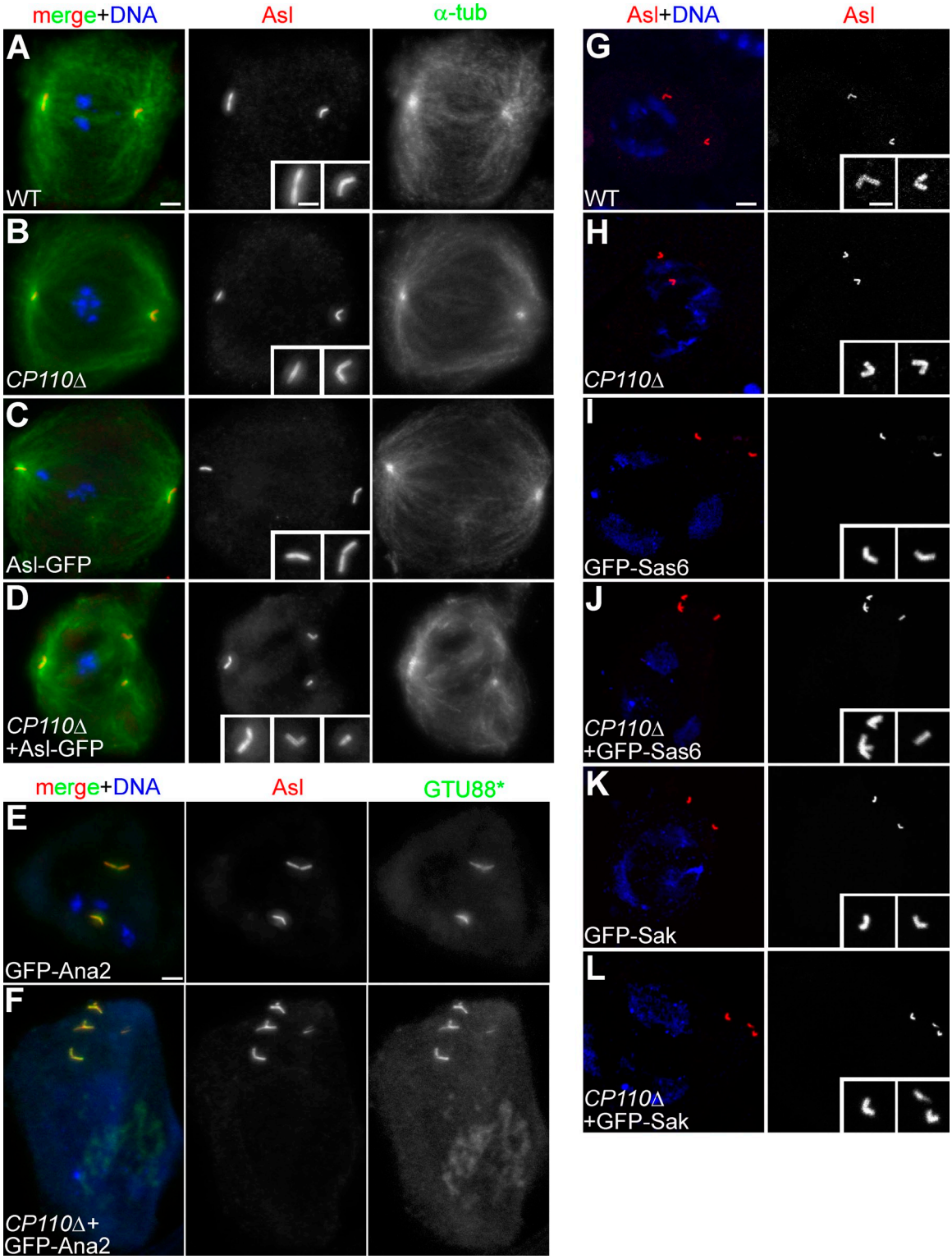

Figure S5. **Centrioles frequently overduplicate in *CP110Δ* primary spermatocytes overexpressing centriole duplication proteins.** (A–D) Panels show WT (A), *CP110Δ* (B), Asl-GFP–overexpressing (C), and *CP110Δ* Asl-GFP–overexpressing (D) primary spermatocytes in meiosis I stained for Asl (red, magnified in insets), α-tubulin (green), and DNA (blue in merged image). WT, *CP110Δ*, and Asl-GFP–overexpressing cells contain two centriole pairs, whereas *CP110Δ* Asl-GFP–overexpressing cells often contain more than four centrioles (in this case two centriole pairs and an extra centriole). (E and F) GFP-Ana2–overexpressing and *CP110Δ* GFP-Ana2–overexpressing primary spermatocytes in G2 phase stained for Asl (red), GTU88* (green), and DNA (blue in merge). GFP-Ana2–overexpressing cells have four centrioles, whereas *CP110Δ* GFP-Ana2–overexpressing cells often have more than four centrioles that are usually arranged in a rosette. (G–L) WT (G), *CP110Δ* (H), GFP-DSas-6–overexpressing (I), *CP110Δ* GFP-DSas-6–overexpressing (J), GFP-Sak–overexpressing (K), and *CP110Δ* GFP-Sak–overexpressing (L) primary spermatocytes in G2 phase stained for Asl (red) and DNA (blue in merge). WT, *CP110Δ*, GFP-DSas-6–overexpressing, and GFP-Sak–overexpressing cells contain two centriole pairs, whereas *CP110Δ* GFP-DSas-6–overexpressing and *CP110Δ* GFP-Sak–overexpressing cells often contain more than four centrioles (one centriole pair, a centriole triplet, and an extra centriole [J] or two centriole pairs and an extra centriole [L]). Bars, 5 µm (2.5 µm in insets).

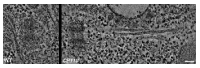

Video 1. **CP110 regulates the length of the centriolar MTs.** Movies show electron tomograms of centrioles in longitudinal orientation in WT (left) and *CP110Δ* (right) third instar larval wing disc cells. Tilt series of 150-nm thick sections were collected from −55° to 55° with 1° angular increment in a transmission electron microscope (TECNAI T12; FEI) at 13,000× using SerialEM (Mastronarde, 2005). Tomograms were reconstructed by R-weighted back projection with the user interphase eTomo and rendered three-dimensional using the IMOD package (Kremer et al., 1996). Centrioles were oriented along their longitudinal axis. Each movie frame in the tomogram is a projection of 10 individual slices. Note that centriolar MTs are dramatically elongated in the absence of CP110, and these extensions consist largely of single MTs. Bar, 100 nm.

Video 2. **CP110 regulates the length of the centriolar MTs in S2 cells.** Movies show electron tomograms of centrioles in longitudinal orientation in S2 cells treated with GFP (control, left) and CP110 (right) RNAi. Tilt series of 150-nm thick sections were collected from −55° to 55° with 1° angular increment in a transmission electron microscope (TECNAI T12; FEI) at 13,000× using SerialEM (Mastronarde, 2005). Tomograms were reconstructed by R-weighted back projection with the user interphase eTomo and rendered three-dimensional using the IMOD package (Kremer et al., 1996). Centrioles were oriented along their longitudinal axis. Each movie frame in the tomogram is a projection of 10 individual slices. Note how long singlet and doublet MT extensions can be seen in the CP110-depleted centriole. Bar, 100 nm.

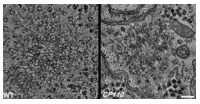

Video 3. **MT singlets elongate from *CP110Δ* centrioles.** Movies show electron tomograms of centrioles in cross section in WT (left) and *CP110Δ* (right) third instar larval brain cells. Tilt series of 150-nm thick sections were collected from −55° to 55° with 1° angular increment in a transmission electron microscope (TECNAI T12; FEI) at 13,000× using SerialEM (Mastronarde, 2005). Tomograms were reconstructed by R-weighted back projection with the user interphase eTomo and rendered three-dimensional using the IMOD package (Kremer et al., 1996). Each movie frame in the tomogram is a projection of 10 individual slices. The MT protrusions from the *CP110Δ* centriole are predominantly singlets rather than doublets. Bar, 100 nm.

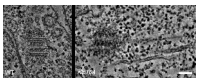

Video 4. **Klp10A regulates the length of the centriolar MTs.** Movies show electron tomograms of centrioles in longitudinal orientation in WT (left) and *Klp10A* (right) third instar larval wing disc cells. Tilt series of 150-nm thick sections were collected from −55° to 55° with 1° angular increment in a transmission electron microscope (TECNAI T12; FEI) at 13,000× using SerialEM (Mastronarde, 2005). Tomograms were reconstructed by R-weighted back projection with the user interphase eTomo and rendered three-dimensional using the IMOD package (Kremer et al., 1996). Centrioles were oriented along their longitudinal axis. Each movie frame in the tomogram is a projection of 10 individual slices. Note that the WT electron tomogram is the same as that shown in Video 1, and it is shown again here simply for ease of comparison. Centriolar MTs are dramatically elongated in the *Klp10A* mutant centriole, and these extensions consist largely of doublet MTs. Bar, 100 nm.

Table S1. **PCR primer list**

Name	Orientation	Sequence	Binding region
AF8	For	GAATTCGGCCAGCTGTTTCAAA	Upstream of *CP110* 5′UTR
AF9	Rev	TTGACGTTGGCTGCACTTCAT	PBac{RB}Cp110[e00667]
AF10	For	GACAGTACTGAAGAGCCAGTAA	PBac{RB}Cp110[e00667]
AF11	Rev	TGCTGCAGCTGTGACACACTT	Beginning of *CP110* coding region
AF12	For	GGGTAGATTCGGTAGTATCCTT	*CP110* 3′UTR
AF13	Rev	ACCTAACGCACAGTCACGTTA	P{XP}l(1)G0196[d05025]
AF14	For	GTATAAATAGAGGCGCTTCGTCT	P{XP}l(1)G0196[d05025]
AF15	Rev	GTAGGAGGCGGAGGAAGAGAA	Downstream of *CP110* 3′UTR
AF18	For	GATTCAGCTGACCTCTGAGAAG	*CP110* 5′UTR
AF21	For	CCATTATAGCGAAAAGGGGAAG	Middle of *CP110* coding region
AF22	Rev	GAATGGGAGTACAGGAAATAGAT	Middle of *CP110* coding region
AF23	For	TAATGGGTAGATTCGGTAGTATC	*CP110* 3′UTR
AF24	Rev	GAATTATGGAATTGGGTGGGCA	*CP110* 3′UTR

Table S2. **PCRs to assess the deletion of CP110 in the CP110Δ mutant stocks (products obtained using the following primer pairs and DNA)**

Primer pair	WT	PBac{RB}Cp110[e00667]	P{XP}l(1)G0196[d05025]	CP110Δ	Binding region
AF18 + AF11	556 bp	556 bp	556 bp	No product	*CP110* 5′UTR and beginning of *CP110* coding region
AF21 + AF22	745 bp	745 bp	745 bp	No product	Middle of *CP110* coding sequence
AF23 + AF24	511 bp	511 bp	511 bp	No product	*CP110* 3′UTR
AF8 + AF9	No product	1024 bp	No product	1024 bp	Upstream of *CP110* 5′UTR and beginning of PBac{RB}Cp110[e00667]
AF10 + AF11	No product	1090 bp	No product	No product	End of PBac{RB}Cp110[e00667] and beginning of *CP110* coding region
AF12 + AF13	No product	No product	1057 bp	No product	*CP110* 3′UTR and beginning of P{XP}l(1)G0196[d05025]
AF14 + AF15	No product	No product	994 bp	994 bp	End of P{XP}l(1)G0196[d05025] and downstream of *CP110* 3′UTR

References

Kremer, J.R.J., D.N.D. Mastronarde, and J.R.J. McIntosh. 1996. Computer visualization of three-dimensional image data using IMOD. *J. Struct. Biol.* 116:71–76. http://dx.doi.org/10.1006/jsbi.1996.0013

Mastronarde, D.N. 2005. Automated electron microscope tomography using robust prediction of specimen movements. *J. Struct. Biol.* 152:36–51. http://dx.doi.org/10.1016/j.jsb.2005.07.007